Structural Comparisons of Apo- and Metalated Three-Stranded Coiled Coils Clarify Metal Binding Determinants in Thiolate Containing Designed Peptides

Saumen Chakraborty,[†] Debra S. Touw,[†,§] Anna F. A. Peacock,[†,⊥] Jeanne Stuckey,[‡] and Vincent L. Pecoraro*,[†]

Department of Chemistry and Life Sciences Institute, University of Michigan, Ann Arbor, Michigan 48109

Received March 3, 2010; E-mail: vlpec@umich.edu

Abstract: Over the past two decades, designed metallopeptides have held the promise for understanding a variety of fundamental questions in metallobiochemistry; however, these dreams have not yet been realized because of a lack of structural data to elaborate the protein scaffolds before metal complexation and the resultant metalated structures which ultimately exist. This is because there are few reports of structural characterization of such systems either in their metalated or nonmetalated forms and no examples where an apo structure and the corresponding metalated peptide assembly have both been defined by X-ray crystallography. Herein we present X-ray structures of two *de novo* designed parallel three-stranded coiled coils (designed using the heptad repeat (**a** → **g**)) **CS**L9C (**CS** = **Coil Ser**) and **CS**L19C in their nonmetalated forms, determined to 1.36 and 2.15 Å resolutions, respectively. Leucines from either position 9 (**a** site) or 19 (**d** site) are replaced by cysteine to generate the constructs **CS**L9C and **CS**L19C, respectively, yielding thiol-rich pockets at the hydrophobic interior of these peptides, suitable to bind heavy metals such as As(III), Hg(II), Cd(II), and Pb(II). We use these structures to understand the inherent structural differences between **a** and **d** sites to clarify the basis of the observed differential spectroscopic behavior of metal binding in these types of peptides. Cys side chains of (**CS**L9C)$_3$ show alternate conformations and are partially preorganized for metal binding, whereas cysteines in (**CS**L19C)$_3$ are present as a single conformer. Zn(II) ions, which do not coordinate or influence Cys residues at the designed metal sites but are essential for forming X-ray quality crystals, are bound to His and Glu residues at the crystal packing interfaces of both structures. These "apo" structures are used to clarify the changes in metal site organization between metalated As(**CS**L9C)$_3$ and to speculate on the differential basis of Hg(II) binding in **a** versus **d** peptides. Thus, for the first time, one can establish general rules for heavy metal binding to Cys-rich sites in designed proteins which may provide insight for understanding how heavy metals bind to metallochaperones or metalloregulatory proteins.

Introduction

Because of the inherent complexity of proteins, it is often difficult to discern the sequence determinants that confer structural stability and function to the biopolymer. Hence, a complete understanding of how a protein's primary amino acid sequence defines its three-dimensional structure and function has eluded many researchers for decades and still it is not very well understood. One approach to simplify this problem is the *de novo* design of model proteins and peptides which are less complex than their natural counterparts, yet contain sufficient information in their sequences to clarify protein structure−function relationships.[1−3] Current studies in protein design are focused on unveiling important structural features in natural protein systems with the ultimate goal of using this knowledge to design novel proteins that are tailor-made to carry out receptor, sensory, and catalytic functions.[4−9] *De novo* design of proteins and metalloproteins has been dominated by α-helical coiled coil and bundle domains; however, secondary structural motifs other than α helices have also been used such as $\beta_2\alpha$,[10−12] small peptides

[†] Department of Chemistry, University of Michigan.
[§] Current Address: Program in Molecular Medicine, University of Massachusetts Medical School, 373 Plantation St., Worcester, Massachusetts 01605.
[⊥] Current Address: University of Birmingham, School of Chemistry, Edgbaston, Birmingham, U.K. B15 2TT.
[‡] Life Sciences Institute, University of Michigan.

(1) Regan, L.; DeGrado, W. F. *Science* **1988**, *241*, 976–978.
(2) DeGrado, W. F.; Wasserman, Z. R.; Lear, J. D. *Science* **1989**, *243*, 622–628.
(3) Bryson, J. W.; Betz, S. F.; Lu, Z. X.; Suich, D. J.; Zhou, H. X. *Science* **1995**, *270*, 935–941.
(4) Tuchscherer, G.; Scheibler, L.; Dumy, P.; Mutter, M. *Biopolymers* **1998**, *47*, 63–73.
(5) Baltzer, L.; Nilsson, J. *Curr. Opin. Biotechnol.* **2001**, *12*, 355–360.
(6) DeGrado, W. F. *Nature* **2003**, *423*, 132–133.
(7) Lu, Y. *Inorg. Chem.* **2006**, *45*, 9930–9940.
(8) Koder, R. L.; Dutton, P. L. *Dalton Trans.* **2006**, 3045–3051.
(9) Kaplan, J.; DeGrado, W. F. *Proc. Natl. Acad. Sci. U.S.A.* **2004**, *101*, 11566–11570.
(10) Krizek, B. A.; Merkle, D. L.; Berg, J. M. *Inorg. Chem.* **1993**, *32*, 937–940.
(11) Struthers, M. D.; Cheng, R. P.; Imperiali, B. *J. Am. Chem. Soc.* **1996**, *118*, 3073–3081.

Table 1. Peptide Sequences Used in This Study[a]

Peptide	Sequence
TRI	Ac-G LKALEEK LKALEEK LKALEEK LKALEEK G-NH$_2$
Grand	Ac-G LKALEEK LKALEEK LKALEEK LKALEEK LKALEEK G-NH$_2$
Coil Ser	Ac-E WEALEKK LAALESK LQALEKK LEALEHG-NH$_2$
CSL9C	Ac-E WEALEKK CAALESK LQALEKK LEALEHG-NH$_2$
CSL19C	Ac-E WEALEKK LAALESK LQACEKK LEALEHG-NH$_2$
CSL16Pen	Ac-E WEALEKK LAALESK LQALEKK LEALEHG-NH$_2$
CSL16DPen	Ac-E WEALEKK LAALESK XQALEKK LEALEHG-NH$_2$

[a] X (red) = Penicillamine. Residues in red indicate substitutions from parent peptides D-Pen = D-Penicillamine.

that bind metal clusters at loop region,[13−15] γ turns,[16] β-hairpin peptides,[17,18] and β sheet structures.[19−21]

Research in our laboratory focuses on the broad areas of heavy metal biochemistry and metalloprotein design. The systems that are used to understand these fundamental issues are the **TRI**,[22] **GRAND**,[23] and **Coil Ser**[24] series of peptides, designed based on the well-known heptad repeat (Table 1 shows the sequences) and form well folded three-stranded parallel coiled coils in solution and solid state. One of our major goals has been to develop models that provide a foundational understanding of the interactions of heavy metals with different metalloregulatory proteins such as MerR, ArsR/Smtb and to develop effective heavy meal sequestering agents. We have reported numerous successes using the *de novo* protein design strategy to further understand heavy metal biochemistry using peptide systems based on the three-stranded coiled coil motif (**TRI** series), including the first water-soluble spectroscopic model of the MerR protein,[25] the first trigonal pyramidal As(III) bound to three cysteines as a model of ArsR[26] (**Coil Ser** series), and the first example of a trigonal thiolate Cd(II).[27,28] From a metalloprotein design perspective, we have provided a quantita-

tive thermodynamic evaluation of Hg(II) binding demonstrating cooperative metalloprotein folding[23] and using the **GRAND** series we have been able to design for the first time hetero-chromic peptides that sequester Cd(II) as 4-coordinate CdS$_3$O at one site and as trigonal planar CdS$_3$ structure at a second site within the same peptide construct.[29,28] The **TRI** and **GRAND** series of peptides are related to V$_a$L$_d$, in which valine occupies all **a** positions and leucine all **d** positions, which was shown[30] using X-ray crystallography to be a parallel three-stranded coiled coil. Substitution of one or more Leu residues from **a** and/or **d** position of **TRI** or **GRAND** peptides with Cys or Penicillamine (Pen) generate thiol-rich sites at the interior of the coiled coil which bind heavy metals such as Hg(II), Cd(II), As(III), Pb(II), and Bi(III).[22,23,25−27,29,31−36] While effective protein based heavy metal sequestering agents, these series of peptides are not easily crystallizable. For structural studies, we have used the structurally similar substituted **Coil Ser** (**CS**) series of peptides (Table 1) which are also based on a heptad repeat, and which can crystallize as parallel or antiparallel three-stranded coiled coils. **Coil Ser** was first crystallized by Lovejoy and DeGrado et al., as an antiparallel coiled coil at low pH.[24] It was suggested that the steric clash between the N-terminal Trp residues led to the antiparallel orientation. Subsequent NMR work demonstrated that **Coil Ser** formed parallel three-stranded coiled coils in slightly basic solution.[37] We have subsequently characterized both metalated and apo derivatives of **Coil Ser** peptides which have been shown to be parallel three-stranded coiled coils. This orientation may reflect the pH, the sequence modification, the presence of metals bound in the hydrophobic interior, the presence of Zn(II) ions that bind to external His and Glu residues at the crystal packing interfaces or a combination of these factors.[26,38]

Despite the fact that there are a significant number of studies using *de novo* designed peptide systems by many different groups, there are only few examples of structurally characterized *de novo* designed constructs available in the literature. The most well characterized systems are four helix bundle motifs consisting of dimers of helix-turn-helix peptides known as Dueferri (DF), designed by DeGrado. These peptides serve as paradigms for di-iron, dizinc, and dimanganese containing natural proteins and contain carboxylate (Glu) bridged dinuclear metal sites at the center of the four helix bundle.[39] Various Zn(II), Cd(II), and Mn(II) derivatives of DF have been characterized crystallograph-

(12) Struthers, M. D.; Cheng, R. P.; Imperiali, B. *Science* **1996**, *271*, 342–345.
(13) Hill, C. L.; Steenkamp, D. J.; Holm, R. H.; Singer, T. P. *Proc. Natl. Acad. Sci. U.S.A.* **1977**, *74*, 547–551.
(14) Gibney, B. R.; Rabanal, F.; Skalicky, J. J.; Wand, A. J.; Dutton, P. L. *J. Am. Chem. Soc.* **1999**, *121*, 4952–4960.
(15) Daugherty, R. G.; Wasowicz, T.; Gibney, B. R.; DeRose, V. J. *Inorg. Chem.* **2002**, *41*, 2623–2632.
(16) Bonomo, R. P.; Casella, L.; Gioia, L. D.; Molinari, H.; Impellizzeri, G.; Jordan, T.; Pappalardo, G.; Rizzarelli, E. *J. Chem. Soc., Dalton Trans.* **1997**, 2387–2389.
(17) Cheng, R. P.; Fisher, S. L.; Imperiali, B. *J. Chem. Soc., Dalton Trans.* **1996**, *118*, 11349–11356.
(18) Rosenblatt, M. M.; Wang, J. Y.; Suslick, K. S. *Proc. Natl. Acad. Sci. U.S.A.* **2002**, *100*, 13140–13145.
(19) Schneider, J. P.; Kelly, J. W. *J. Am. Chem. Soc.* **1995**, *117*, 2533–2546.
(20) Platt, G.; Chung, C.; Searle, M. *Chem. Commun.* **2001**, 1162–1163.
(21) Venkatraman, J.; Naganagowda, G. A.; Sudha, R.; Balaram, P. *Chem. Commun.* **2001**, 2660–2661.
(22) Dieckmann, G. R.; McRorie, D. K.; Lear, J. D.; Sharp, K. A.; DeGrado, W. F.; Pecoraro, V. L. *J. Mol. Biol.* **1998**, *280*, 897–912.
(23) Ghosh, D.; Pecoraro, V. L. *Inorg. Chem.* **2004**, *43*, 7902–7915.
(24) Lovejoy, B.; Choe, S.; Cascio, D.; McRorie, D.; DeGrado, W.; Eisenberg, D. *Science* **1993**, *259*, 1288–1293.
(25) Dieckmann, G. R.; McRorie, D. K.; Tierney, D. L.; Utschig, L. M.; Singer, C. P.; O'Halloran, T. V.; Penner-Hahn, J. E.; DeGrado, W. F.; Pecoraro, V. L. *J. Am. Chem. Soc.* **1997**, *119*, 6195–6196.
(26) Touw, D. S.; Nordman, C. E.; Stuckey, J. A.; Pecoraro, V. L. *Proc. Natl. Acad. Sci. U.S.A.* **2007**, *104*, 11969–11974.
(27) Lee, K.-H.; Cabello, C.; Hemmingsen, L.; Marsh, E. N. G.; Pecoraro, V. L. *Angew. Chem., Int. Ed.* **2006**, *45*, 2864–2868.
(28) Peacock, A. F. A.; Hemmingsen, L.; Pecoraro, V. L. *Proc. Natl. Acad. Sci. U.S.A.* **2008**, *105*, 16566–16571.

(29) Iranzo, O.; Cabello, C.; Pecoraro, V. L. *Angew. Chem., Int. Ed.* **2007**, *46*, 6688–6691.
(30) Ogihara, N. L.; Weiss, M. S.; DeGrado, W. F.; Eisenberg, D. *Protein Sci.* **1997**, *6*, 80–88.
(31) Farrer, B.; McClure, C.; Penner-Hahn, J. E.; Pecoraro, V. L. *Inorg. Chem.* **2000**, *39*, 5422–5423.
(32) Farrer, B. T.; Harris, N. P.; Balchus, K. E.; Pecoraro, V. L. *Biochemistry* **2001**, *40*, 14696–14705.
(33) Farrer, B.; Pecoraro, V. L. *Proc. Natl. Acad. Sci. U.S.A.* **2003**, *100*, 3760–3765.
(34) Matzapetakis, M.; Farrer, B. T.; Weng, T.-C.; Hemmingsen, L.; Penner-Hahn, J. E.; Pecoraro, V. L. *J. Am. Chem. Soc.* **2002**, *124*, 8042–8054.
(35) Matzapetakis, M.; Ghosh, D.; Weng, T.-C.; Penner-Hahn, J. E.; Pecoraro, V. L. *J. Biol. Inorg. Chem.* **2006**, *11*, 876–890.
(36) Matzapetakis, M.; Pecoraro, V. L. *J. Am. Chem. Soc.* **2005**, *127*, 18229–18233.
(37) Wendt, H.; Berger, C.; Baici, A.; Thomas, R. M.; Bosshard, H. R. *Biochemistry* **1995**, *34*, 4097–4107.
(38) Peacock, A. F. A.; Stuckey, J. A.; Pecoraro, V. L. *Angew. Chem., Int. Ed.* **2009**, *48*, 7371–7374.
(39) Calhoun, J. R.; Nastri, F.; Maglio, O.; Pavone, V.; A.;, L.; DeGrado, W. F. *Peptide Sci.* **2005**, *80*, 264–278.

ically.[40−42] To determine the extent to which the active site is preorganized in the absence of metals, NMR structure of apo DF1 was solved which suggested that the native fold and metal binding site are largely preorganized in the apo protein.[43] Active sites of metalloproteins are frequently preorganized in the absence of metals, which requires burial of polar amino acids at the interior at the expense of folding free energy.[44] Preorganization requires that proteins impart their own structural preference on metals to bind in a specific geometry.

We have been directing our efforts toward the structural characterization of various three-stranded coiled coils. Recently, we reported the X-ray structure[26] of As(CSL9C)₃ where As(III) is coordinated to three Cys residues in an endo conformation within a protein environment. This construct served as the first structural model for As(III) binding to ArsR or ArsD.[45,46] We have also successfully obtained the structures of both L- and D-versions of unmetalated (apo) Pen derivatives (CSL16-L-Pen and CSL16-D-Pen) which are both substituted in the **a** heptad position.[38] The sulfur atoms of L-thiol containing residues appear to be orientated in a similar way when the mutation occurs at an **a** site and appear to be independent of both the place of substitution in the coiled coil, 9 versus 16, the nature of the coordinating ligand, L-Cys versus L-Pen, as well as the state of metalation. A comparison of the structures of apo (CSL16-L-Pen)₃ and metalated As(CSL9C)₃ show that the sulfurs appear to be preorganized for metal binding. The major differences in the Pen versus Cys structures are the packing of the two methyl groups on the Pen. The plane below the Cys is blocked by one set of methyl groups which point toward the interior of the coiled coil below the sulfurs, the second set of methyl groups points away from the center in-between the helical interfaces. The D-Pen points down toward the C-terminus and most interestingly appears to point away from the interior of the coiled coil toward the helical interfaces. The dramatically different Cd(II) binding to CSL16-L-Pen and CSL16-D-Pen has been correlated with the structural differences. Furthermore, we have demonstrated that the affinities and selectivities of metal binding to **a** versus **d** site substituted peptides are different in solution.[36,47] Cd(II) binds selectively to **a** site and has 10-fold higher binding affinity over **d** site.[34] Pb(II), on the other hand, has 4 times higher affinity for binding to **d** site over **a** site.[48] Evidently, structural information about **a** and **d** sites within these coiled coils is sorely required.

In this article, we present the structures of two apo peptides, (CSL9C)₃ which is an **a** site peptide, and (CSL19C)₃ which is a **d** substituted peptide. With the apo structure of the **a** site peptide (CSL9C)₃, we address local/global structural differences with the metalated analogue As(CSL9C)₃,[26] effect of arsenic binding on the overall structure of the peptide and answer questions as to whether As(III) binding changes significantly the conformation of the coordinating Cys residues, the extent of the degree of preorganization of the coordinating residues at the metal binding site and finally whether large amounts of water are extruded on metal coordination. The structure of apo (CSL9C)₃ now provides a comprehensive basis for a direct comparison of the metalated and apo three-stranded coiled coils in these types of designed polypeptide systems. The apo (CSL19C)₃ structure enables us to address whether there are major conformational differences between the orientation of Cys sulfurs in **a** versus **d** sites, which thiol site generates more void space in the hydrophobic interior, how different are the packing of hydrophobes above and below the Cys site, and what are the consequences of the observed differences. The (CSL9C)₃ structure shows that the Cys side chains have conformational flexibility and the orientation is partitioned between the coiled coil interior and helical interface. On the basis of the structural analysis of these two apo peptides, we also hypothesize possible modes in which Hg(II) would coordinate to these peptides. With the knowledge gained from this study, we now have access to the rules for the *de novo* design of metal binding sites within the interior of coiled coils, as well as a deeper understanding of heavy metal binding in designed proteins, potentially providing significant insight into metal binding in metalloregulatory proteins and metallochaperones.

Results

Overall Structure. The X-ray structures of well-folded, three-stranded parallel coiled coil peptides (CSL9C)₃ and (CSL19C)₃ have been determined to 1.36 and 2.15 Å resolution, respectively. The final model of (CSL9C)₃ contains 816 protein atoms, 59 water molecules, 5 Zn(II) ions, 1 Ca(II) ion, and 3 ethylene glycol molecules. (CSL19C)₃ contains 699 protein atoms, 19 water molecules, and six Zn(II) ions. The rmsd between the 29 amino acids of CSL16-L-Pen (PDB code 3H5F)[38] as the search model and the final refined structure of (CSL9C)₃ is 0.024 Å. Leu 9 of CSL16-L-Pen was mutated to Cys and the side chains of Pen 16 were modified in such a way that they resembled Leu residues containing only Cβ and Cγ atoms before using it as a search model for Molecular Replacement. After one round of refinement, the methyl groups of Leu were built in using the density present in $F_o − F_c$ electron density map. Using the first 26 amino acids of the single helix of Coil V_aL_d (PDB code 1COI)[30] as the search model, the rmsd for the final refined structure of (CSL19C)₃ is 0.025 Å. All nonglycine residues for both the structures fall in the right handed α-helical region of the Ramachandran plot.[49] The carbonyls of N-terminal capping acetyl groups in both structures are hydrogen bonded to Ala 4 of respective main chains. In (CSL9C)₃, the amide NH₂ groups of chains A and C are hydrogen bonded to the main chain CO of Ala 25 from respective chains. All side chains in both the structures except those involved in metal binding or hydrogen bonding to solvent molecules are present in their preferred rotameric conformation as analyzed by rotamer check utility in Coot.[50]

(40) Lombardi, A.; Summa, C. M.; Geremia, S.; Randaccio, L.; Pavone, V.; DeGrado, W. F. *Proc. Natl. Acad. Sci. U.S.A.* **2000**, *97*, 6298–6305.

(41) Lahr, S. J.; Engel, D. E.; Stayrook, S. E.; Maglio, O.; North, B.; Geremia, S.; Lombardi, A.; DeGrado, W. F. *J. Mol. Biol.* **2005**, *346*, 1441–1454.

(42) Costanzo, L. D.; Wade, H.; Geremia, S.; Randaccio, L.; Pavone, V.; DeGrado, W. F.; Lombardi, A. *J. Am. Chem. Soc.* **2001**, *123*, 12749–12757.

(43) Maglio, O.; Nasti, F.; Pavone, V.; Lombardi, A.; DeGrado, W. F. *Proc. Natl. Acad. Sci. U.S.A.* **2003**, *100*, 3772–3777.

(44) Pasternak, A.; Kaplan, J.; Lear, J. D.; Degrado, W. F. *Protein Sci.* **2001**, *10*, 958–969.

(45) Shi, W.; Dong, J.; Scott, R. A.; Ksenzenko, M. Y.; Rosen, B. P. *J. Biol. Chem.* **1996**, *271*, 9291–9297.

(46) Lin, Y.-F.; Yang, J.; Rosen, B. P. *J. Biol. Chem.* **2007**, *282*, 16783–16791.

(47) Matzapetakis, M. Ph.D. Thesis, University of Michigan, Ann Arbor, MI, 2005; p 249.

(48) Touw, D. S. Ph.D. Thesis, University of Michigan, Ann Arbor, MI, 2007.

(49) Ramachandran, G. N.; Ramakrishnan, C.; Sasisekharan, V. *J. Mol. Biol.* **1963**, *7*, 95–99.

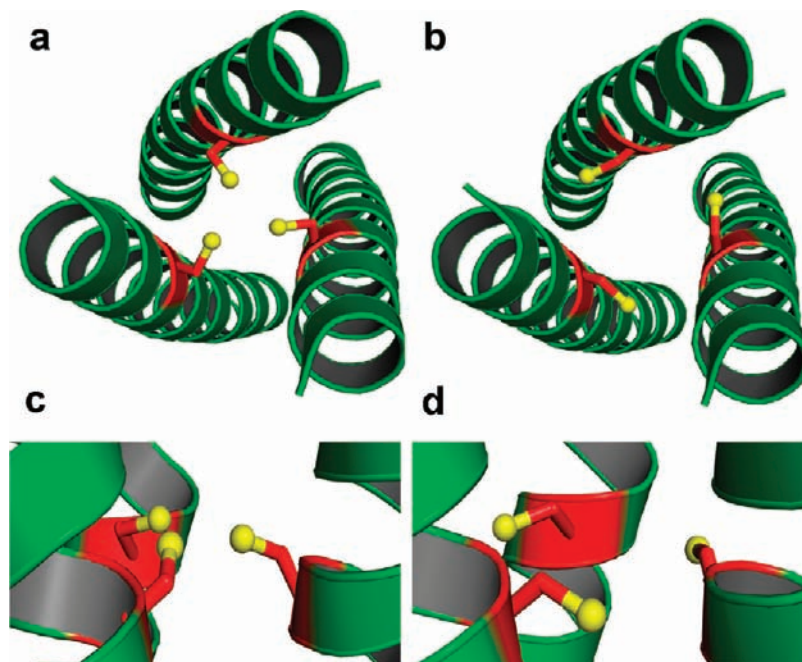(50) Emsley, P.; Cowtan, K. *Acta Crystallogr., Sect. D* **2004**, *60*, 2126–2132.

Figure 1. Ribbon diagrams of (**CSL9C**)$_3$ showing the orientation of Cys side chains. Main chain atoms are shown as green ribbon and the Cys side chain as red stick with the thiol groups being shown as yellow spheres. Top-down view from N-termini showing the exclusive orientation of the (a) major conformer (15%) where all the Cys side chains are pointing toward the interior of the coiled coil and (b) minor conformer (10%) where all Cys side chains are oriented toward the helical interface. Side views show that the thiol groups are pointing toward the N- termini and C-termini of the helical scaffold in the interior (c) and (d) exterior Cys conformers, respectively.

Cysteine Sites. Side chains of all three cysteine residues of **CSL9C** display alternate conformations. The cysteine side chains in all three helices are oriented in essentially equal proportion between the coiled coil interior and the helical interface (in chain C, the cysteine side chain is oriented toward the interior and helical interface at what is best modeled as a 60:40 ratio). Thus, there is an ensemble of different combinations of cysteine side chain orientations between three peptide helices. Out of these different orientations of three Cys side chains, 15% (0.5 × 0.5 × 0.6 × 100%) of the time all the cysteine side chains are exclusively oriented toward the interior of the coiled coil and 10% of the time all of them are oriented toward the helical interface. The orientations of the two conformers of Cys residues are shown in Figure 1. The separation between the S$_\gamma$ atoms (S−S) of the three cysteines for the interior conformation is 3.32 Å, whereas the S$_\gamma$ atoms for the exterior conformation are separated at a distance of 6.85 Å with respect to each other. It can be seen from Figure 1 that the thiol groups of cysteine side chains in the interior conformation are directing toward the N-termini of the helices, whereas those in the exterior conformation are pointing toward the C-termini. The distance between the planes formed by the S$_\gamma$ atoms of the two conformers of cysteines is 1.11 Å. The β-methylene carbons of all Cys residues are pointing toward the N-terminus of the helical scaffold. The distance between the C$_\alpha$ and C$_\beta$ planes of cysteines is 1.07 Å. The S$_\gamma$ atoms in the interior orientation of cysteines are in a plane which is at a distance of 0.59 Å above from the C$_\beta$ plane of cysteines. On the other hand, the S$_\gamma$ atoms in the exterior orientation of cysteines are in a plane which is 0.52 Å below from the C$_\beta$ plane of cysteines. The χ_1 dihedral angles (N−C$_\alpha$−C$_\beta$−S$_\gamma$) for the interior orientation of cysteines are −70.3 ± 3.9 which are close to the value of −65.2° for most common cysteine rotamers.[51] The χ_1 values for the outer conformer are 171.4° ± 6.2. The leucine layers above (Leu 5) and below (Leu 12) Cys 9, both of which are **d** sites of the

heptad, are oriented differently (Figure 2). Leu 5 is oriented more toward the center of the coiled coil with the Leu 12 layer being oriented away from the center. One methyl group of both Leu 5 and Leu 12 is pointing toward the N-termini and the other one is directing toward the C-termini. The distances between the planes formed by the C$_\gamma$ atom of Leu 5 and Leu 12 and the S$_\gamma$ of interior cysteines conformer are 3.85 and 5.29 Å, respectively. The distances for the exterior cysteine conformer are 4.99 and 4.24 Å from Leu 5 and Leu 12 planes formed by the C$_\gamma$ atoms, respectively.

The orientation of the cysteine side chains in (**CSL19C**)$_3$ is depicted in Figure 3. β-Methylene groups of three cysteines are pointing toward the N-termini. The χ angles for the three cysteines are −90.53°, −165.92°, and 164.33° for chains A, B, and C, respectively. All three cysteines are present as a single rotamer. Thiol groups of both Cys B and C are oriented toward the interior of the helices and toward the C-termini, while Cys A is oriented toward the helical interface and almost perpendicular to the helical axis. The latter orientation toward the helical interface is in accordance with previous predictions[22] which were based on the Coil V$_a$L$_d$ structure.[30] Electron density in the center of the coiled coil corresponding to a heavy atom was not found in $F_o − F_c$ maps down to a contour level of 2σ. The cysteine sulfhydryl groups were found to be greater than 3 Å from one another, excluding the possibility of disulfide bridge formation, which would not be likely at pH 6.5 where the cysteines are more likely to be protonated than deprotonated. The S−S separations for Cys A−Cys B, Cys B−Cys C, and Cys C−Cys A are 4.64, 3.40, and 4.59 Å, respectively.

Noncovalent Interactions. The structure of (**CSL9C**)$_3$ has seven interhelical salt bridge interactions. Glu 3 B forms an intrahelical salt bridge with Lys 7. In addition to interhelical salt bridge interactions between side chains of **e** and **g** residues

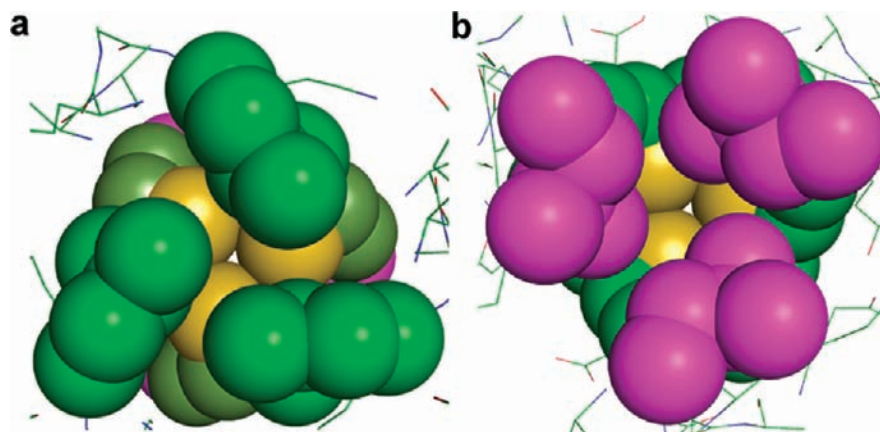(51) Ponder, J. W.; Richards, F. M. *J. Mol. Biol.* **1987**, *193*, 775–791.

Figure 2. Packing of Leu layers above and below the Cys site of **CSL9C** trimer shown as spheres. (a) Top-down view from N-termini, showing the Leu 5 layer (green) and (b) Leu 12 layer (magenta), viewing from C-termini up the helical axis. It shows that metals with stereochemically active lone pair such as As(III) would bind to a coiled coil in an **a** site such that the lone pair would be housed in the open space toward the C-termini.
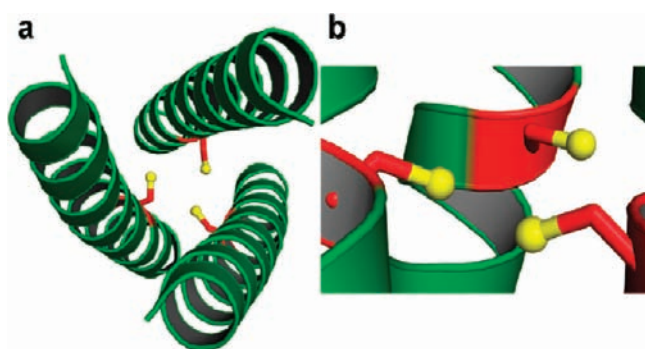

Figure 3. Ribbon diagrams of (**CSL19C**)₃ showing the orientation of Cys side chains. Main chain atoms are shown as green ribbon and the Cys side chain as red sticks with the thiol groups being shown as yellow spheres. (a) Top-down view from N-termini showing that two Cys side chains are pointing toward the interior of the coiled coil with the third thiol directed toward the helical interface. (b) Side view shows that two thiol groups are pointing toward the C-termini of the helical scaffold and the third thiol is almost perpendicular to the helical axis.

Glu and Lys commonly found in coiled coils, there is also an unusual interhelical salt bridge present, between **b** and **g** residues involving Glu 24 A and Lys 22 C. There is an interhelical water mediated hydrogen bonding interaction between Lys 22 A/Glu 20 B. The indole NH of Trp 2 B is involved in hydrogen bonding with Glu 6 B side chain. There are many hydrogen bonding interactions involving side chain and main chains such as, Glu 3 A, and Glu 3 C to main chain NH of same residues, Ser 14 C to the main chain CO of Ala 10 and Ser 14. Finally, there are some intrahelical hydrogen bonds involving side chains such as Glu 20 C to Gln 17 C. There are five interhelical electrostatic interactions in (**CSL19C**)₃. Glu 24 B and Lys 22 B are an example of the **e**−**g** salt bridge typically found in three-stranded coiled coils. An interaction between Glu 1 C and Glu 6 B is mediated by a water molecule. Glu 1 C is hydrogen bonded to Trp 2 B and Glu 1 B is hydrogen bonded to Trp 2 A. Helical wheel diagrams of (**CSL9C**)₃ and (**CSL19C**)₃ summarize these interactions in Figure S1 and S2 of Supporting Information.

External Metal Binding Sites. Four out of the five Zn(II) ions in (**CSL9C**)₃ are bound at the crystal packing interfaces. One of them (ZN1) has its ligands as Glu 24 B (Oε2), His 28 B (Nε2), a water molecule and Glu 24 A (Oε2) from a symmetry related peptide trimer. The other Zn(II) (ZN2) is bound to His 28 A (Nε2) and Glu 3 B (Oε1,A/Oε2,B), Glu 20 B (Oε1) and

Glu 24 B (Oε1) from a symmetry related peptide molecule. ZN3 is bound to Glu 1 B (Oε2), Glu 6 C (Oε2), and two water molecules. ZN4 has two water molecules, Glu 6 A (Oε1) and His 28 C (Nε2) from a symmetry related molecule as its ligands. ZN5 is bound to one water molecule, His 28 B (Nδ1), and Glu 20 A (Oε2) from a symmetry related trimer. The Ca(II) ion is bound to Glu 1 A (Oε2) and Glu 6 B (Oε1, Oε2).

Zn(II) ion sites at the crystal packing interfaces of (**CSL19C**)₃ are very different than those of (**CSL9C**)₃. The 6-fold screw axis and crystal packing of the structure is shown in Figure S3 in Supporting Information. There are six Zn(II) ions per asymmetric unit, which form two dinuclear Zn(II) sites and two other Zn(II) ions not directly connected by side chain ligands that are 7.6 Å apart. Detailed views of the Zn(II) binding sites are shown in Figure S4 in Supporting Information. The first site, shown in Panel B which is not dinuclear, has one Zn(II) ion coordinated by Glu 27 C, Glu 24 C, and Lys 22 B from one molecule and Glu 3A from another trimer. The neighboring Zn(II) ion is coordinated by His 28 C from one trimer and Glu 1 C and Glu 6 A from another trimer plus one water molecule. The dinuclear Zn(II) site in Panel C contains a bridging glutamate, Glu 6 B, and the coordination sphere of one Zn(II) ion is filled by His 28 A and Glu 24 A from one helix as well as Glu 1 A from the same trimer as Glu 6 B. The other Zn(II) ion of this cluster is coordinated by Glu 3 B, and weakly coordinated by Glu 24 A and the other carbonyl oxygen of Glu 6 B. All three tryptophan residues are closely associated with the Zn(II) sites on the exterior, and are hydrogen bonded to the Zn(II) ligands. The indole nitrogen of Trp 2 A, Trp 2 B, and Trp 2 C are all 3.8−4.2 Å from a Zn(II) ion.

Discussion

The nomenclature used to define our "apo" and "metalated" peptides is given in ref 52.

(**CSL9C**)₃ and As(**CSL9C**)₃. The α-helical backbones of apo and As(III) bound **CSL9C** are extremely similar and, as shown in Figure 4, overlay very well. This observation demonstrates that As(III) binding does not perturb the overall secondary structure of the coiled coil. Both the apo and As(**CSL9C**)₃ crystallize with 4 Zn(II) ions at the crystal packing interfaces coordinated to His and Glu ligands. In the As(**CSL9C**)₃ structure, all four Zn(II) ions in the asymmetric unit are present at the crystal packing interfaces, whereas in apo (**CSL9C**)₃, four (ZN1, ZN2, ZN4, and ZN5) out of five Zn(II) ions in the
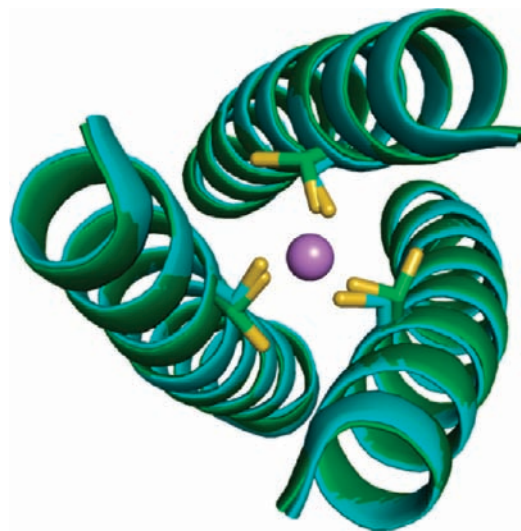
Figure 4. Ribbon diagram showing top-down view of an overlay of apo (**CS**L9C)$_3$ (green) and As(**CS**L9C)$_3$ (cyan) structures. Cysteine side chains are shown in stick form with As(III) as purple sphere. It can be noted that there is no change in the overall secondary structures of apo and metalated peptide. The major change can be noted from the apo structure where Cys side chains are present as alternate conformers which is locked into a single conformer in As(**CS**L9C)$_3$ upon metal binding.

asymmetric unit are bound at the crystal packing interfaces. The same number of interhelical electrostatic interactions are present in (**CS**L9C)$_3$ as there are in As(**CS**L9C)$_3$ except the interaction between Glu 6 B and Glu 1 C which is present only in the latter structure.[26] The β methylene carbons of both the apo and metalated (**CS**L9C)$_3$ structures are pointing toward the N-termini of the helices. The thiol groups of As(**CS**L9C)$_3$ and the major interior conformer of (**CS**L9C)$_3$ are pointing toward the N-termini, with the S−S separation for the major conformer of apo (**CS**L9C)$_3$ being 3.32 Å, which is 0.07 Å longer than the metalated peptide (3.25 Å). The χ_1 dihedral angles for the metalated construct are −60° ± 1 as opposed to −70.3° ± 3.9

(52) **Nomenclature**: While previously describing in detail the nomenclature for peptide modifications, we have not fully provided descriptors for metal complexation to these peptides. We will provide these definitions here with respect to Cd(II) and the exogenous ligand water; however, the nomenclature is general for any metal or nonprotein bound ligand. We refer to an "apo peptide" as one which does not have metal in the designed metal coordination site within the hydrophobic interior of the coiled coils. We do not refer to an "apo peptide" to represent situations without the presence of any cofactors. Metals that may be bound nonspecifically to the exterior hydrophilic residues are not considered to be metalated proteins/peptides in this context. Cd(II)-(TRIL16C)$_3$⁻ indicates that Cd(II) is bound to the three-stranded coiled coil; however, the metal coordination environment is either unknown or is a mixture of species (e.g., Cd(II)(TRIL16C)$_3$⁻ contains a 55:45 mixture of CdS$_3$O and CdS$_3$, respectively). When the metal is placed within brackets, as in [Cd(II)(H$_2$O)](TRIL12AL16C)$_3$⁻, we specify the coordination environment (in this case CdS$_3$O) and the possible exogenous ligand (here water). If the site has only protein ligands, then it would be represented as [Cd(II)](TRIL16Pen)$_3$⁻. At low pH, one can encounter the situation where the cysteine sulfurs are protonated and may, or may not, be directly coordinated to the metal. In this case, we indicate this situation as [Cd(II)](TRIL16Pen[S,(SH)$_2$])$_3$⁻ in which one cysteine is bound as a thiolate and the remaining two cysteines are protonated. When a peptide contains more than one binding site, we use the above nomenclature, but specify which site is being discussed by adding a superscript outside of the bracket to indicate the amino acid residues coordinating the specific metal (e.g., [Cd(II)]¹⁶[Cd(II)(H$_2$O)]³⁰(GRANDL16PenL26AL30C)$_3$⁻²). Finally for cases where dual site peptides exhibit specificity for metal complexation, we will utilize [apo] to designate an empty site (e.g., [apo]¹⁶[Cd(II)(H$_2$O)]³⁰(GRANDL16PenL26AL30C)$_3$⁻).

for the major conformer of the apo structure. Smaller S−S separation and χ_1 dihedral angles in As(**CS**L9C)$_3$ compared to the apo structure where all cysteines are oriented toward the interior suggests that the metal binding induces only minor changes in the geometry of the cysteine residues, making them slightly more constrained upon metal binding. The major change, however, is observed in the conformations of cysteine side chains in the metalated structure compared to the apo peptide where the cysteines are orientated toward the helical interface. The apo structure shows sufficient conformational flexibility of the cysteine side chains as out of an ensemble of many different orientations of Cys side chains, only 15% of the time all the cysteines are exclusively oriented in a conformation where they are preorganized for metal binding. It may, however, be noted that the 15% population of preorganized Cys conformers for metal binding is observed in the solid state where the protein is 45% hydrated (Matthews Coefficient 2.25) and it may not necessarily represent situations that may be occurring in solution. The rapid motion between different cysteine conformers results in favorable entropic contribution in the apo structure. Upon metal binding, this local conformational motion is restricted to a single cysteine conformer which makes the process entropically unfavorable. Moreover, there is reorganization energy required to orient the thiols to the interior for metal binding. The entropic penalty and the cost of required reorganization energy is overcome by the enthalpic gain upon formation of bonds between the soft thiolate ligands and the As(III) ion. The smaller size of As(III) with ionic radius of 0.72 Å fits well within the smaller cavity generated by the interior cysteine conformer resulting in As−S bond distance of 2.28 Å and mean S−As−S angle of 89°.[26] Because of these geometrical restraints, As(III) binding is not suitable to the exterior cysteine conformer. It may be noted that when Cys in an **a** site is replaced by its bulkier analogue Pen (β, β dimethyl cysteine) in **CS**L16-L-Pen the thiol groups of the major rotamer (95%) are found to be positioned toward the interior of the coiled coil preorganized for metal binding. Improved packing of the methyl groups and restricted rotation due to the additional sterics of the bulky methyl groups are believed to lead to this enhanced preorganization and rigidity of the thiols.[38] This begins to explain the different metal binding properties of Cys versus Pen sites that we have observed in solution with various metal ions.

The degree of preorganization of metal binding ligands in metalloproteins varies depending on the functional requirement of the protein active site. Zinc finger proteins feature a metal binding site where Zn(II) binding induces overall folding of the protein.[53] On the contrary, the R2 subunit of ribonucleotide reductase displays significantly smaller geometrical changes around metal binding region in the apo versus different dimetalated forms.[54−56] Structural comparison between As(**CS**L9C)$_3$ and (**CS**L9C)$_3$ shows that As(III) binding does not induce folding of the overall secondary structures of the peptide, but the metal binding thiolate ligands in the apo structure show significant local conformational motion which is restricted upon metal binding and locked into a single conformation. The observed dynamics of Cys side chains in the apo structure

(53) Berg, J. M. *Acc. Chem. Res.* **1995**, *28*, 14–19.
(54) Logan, D. T.; deMare, F.; Persson, B. O.; Slaby, A.; Sjoberg, B.-M.; Nordlund, P. *Biochemistry* **1998**, *37*, 10798–10807.
(55) Andersson, M. E.; Hogbom, M.; Rinaldo-Matthis, A.; Andersson, K. K.; Sjoberg, B.-M.; Nordlund, P. *J. Am. Chem. Soc.* **1999**, *121*, 2346–2352.
(56) Atta, M.; Nordlund, P.; Aberg, A.; Eklund, H.; Fontecave, M. *J. Biol. Chem.* **1992**, *267*, 20682–20688.
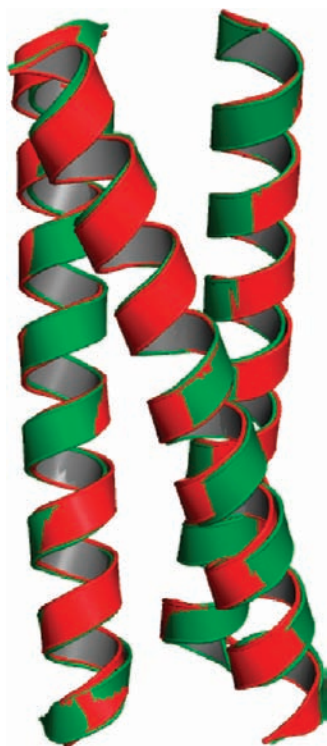
Figure 5. Ribbon diagram showing the overlay of apo (**CS**L9C)₃ (green) and (**CS**L19C)₃ (red). The secondary structures in both the constructs are unperturbed.

suggests a mechanism for insertion of metals into the hydrophobic interior of coiled coils and helical bundles. Initial binding of a metal to a ligand such as cysteine located at the helical interface followed by a breathing motion of the helices coupled with the movement of the amino acid side chain to the interior conformer would internalize the metal within the protein's hydrophobic core.

Intriguingly, the Leu layers above and below the Cys 9 site are oriented in a similar way in both the apo and metalated (**CS**L9C)₃ structures. The Leu 5 layer is tucked in toward the center of the helical axis and the Leu 12 layer is oriented away from the center, thus, opening up space below the metal binding site. It is believed that As(III) binds in a hemidirected endo conformation[26] to (**CS**L9C)₃ so that the stereochemically active

lone pair can be housed in the open space generated by the outward orientation of the Leu 12 layer below Cys 9.

(CSL9C)₃ and (CSL19C)₃. Once again, the peptide backbones of the two apo structures **CS**L9C and **CS**L19C overlay very well as shown in Figure 5. The C_β atoms of cysteines in both the structures are pointing toward the N-termini of the helical scaffold. Cysteine side chains of **CS**L19C appear to be present in single conformers and show sufficient rigidity as opposed to **CS**L9C. The S−S separations in **CS**L19C vary from each other; however, they do generate a larger cavity with which to bind metals with larger ionic radii such as Pb(II). In this structure of **CS**L19C, the cysteines are oriented in such a way that the thiol plane formed by S_γ atoms is not parallel to the planes formed by the C_γ atoms of Leu 16 and Leu 23. The angles between the thiol plane and Leu 16, Leu 23 planes are 8.28° and 3.02°, respectively (Figure S5 in Supporting Information). On the contrary, the thiol plane for **CS**L9C is parallel to Leu 5 and 12. Leucines above and below Cys 19 site are at positions 16 and 23 of the peptide chain and both correspond to **a** sites of the heptad. The Leu residues at the 16 layer are positioned away from the center of the helical axis, whereas those at layer 23 are directing toward the center of the helical axis, see Figure 6. Thus, the Leu 16 layer generates more open space compared to that of the Leu 23 layer. The orientation of these Leu layers above and below the thiol site is exactly opposite compared to that of Leu 5 and Leu 12 of **CS**L9C as mentioned earlier. These differential orientations of Leu layers above and below the cysteine **a** and **d** sites represent one of the important factors that define site selectivity and binding mode preferences of some metals to such sites.

Cys versus Pen Structures. Recently, we have reported the X-ray structures of **CS**L16-L-Pen and its diastereomeric counterpart **CS**L16-D-Pen where the chirality of one amino acid is altered from L- to D- within the coiled coil.[38] Figure S6 in the Supporting Information shows the overlay of the α-helical backbones of the two Cys structures (**CS**L9C, **CS**L19C) and two Pen structures (**CS**L16-L-Pen, **CS**L16-D-Pen). The β-methylene carbons and thiol groups of **CS**L16-L-Pen are oriented toward the N-termini similar to **CS**L9C. Thiol groups of the major rotamer (95%) of each Pen residue in **CS**L16-L-Pen are positioned toward the interior of the coiled coil with S−S separations of 3.7 Å as if preorganized for metal binding like the major rotamer of **CS**L9C (15%, for all Cys side chains).
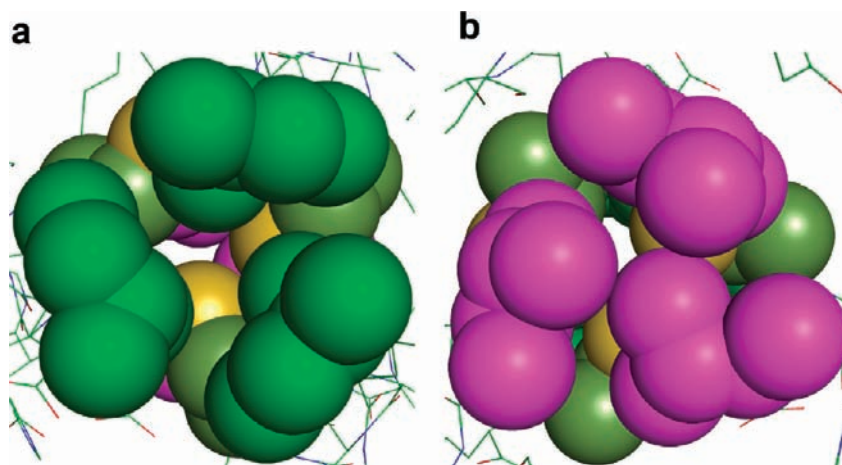

Figure 6. Packing of Leu layers above and below the Cys site of **CS**L19C trimer shown as spheres. (a) Top-down view from N-termini of Leu 16 layer (green) and (b) Leu 23 layer (magenta), viewing from C-termini up the helical axis.

Enhanced degree of preorganization in the Pen structure compared to the Cys structure is believed to be incurred by improved packing of the methyl groups above and below the sulfur plane (one methyl group is pointing toward the N-termini and helical interface whereas the other one is directed toward the C-termini and the interior of the coiled coil) and restricted rotation of the bulky methyl groups. The thiols in the lower abundance rotamers in Pen (5%, each side chain) and Cys (10%, for all side chains) structures are oriented away from the helical axis, toward the helical interface. In **CS**L16-D-Pen, the thiols are directing toward the C-termini similar to the two thiol side chains in **CS**L19C. All the thiols in **CS**L16-D-Pen are positioned away from the helical axis, toward the helical interface, and thus, this site is not preorganized for metal binding within the coiled coil interior. With one thiol group being oriented toward the helical interface in **CS**L19C, the resulting thiol pockets in both D-Pen and **CS**L19C structures are large in general. This analysis suggests that there is some similarity in side chain orientation and the resulting thiol site in **CS**L19C with an L-amino acid in a **d** site and in **CS**L16-D-Pen with a D-amino acid in an **a** site. Because of opposite chirality of D-Pen and L-Cys, the C_β atoms in these two structures are oriented differently. Additionally, the effect of methyl groups in the D-Pen structure might have a significant impact on the observed differential orientation of the thiol groups in the two structures.

Implications of Binding Hg(II). We have shown previously using [199]Hg NMR and [199m]Hg PAC spectroscopic techniques that Hg(II) coordinates to **a** site **TRI** peptides as linear dithiolate HgS_2 complex at the interior of a three-stranded coiled coil at pH 6.5 in the presence of 1:3 ratio of Hg(II)/peptide.[57] This dithiolate−Hg(II) complex is different than Hg(peptide)$_2$ as the presence of a third helix with a protonated cysteine breaks the axial symmetry of the Hg(peptide)$_2$ complex making the Hg(II) adopt a T-shaped geometry. Studies with **d** site peptides also indicate the formation of T-shaped Hg(II) complex at the interior of three-stranded coiled coils under similar conditions (V. L. Pecoraro et al., unpublished results). However, with [199]Hg NMR chemical shift $\delta = -895$ ppm, the **d** site is believed to be more T-shaped than the corresponding **a** site which has a [199]Hg NMR chemical shift $\delta = -908$ ppm. When the pH is raised, a trigonal Hg(peptide)$_3^-$ complex is formed. The conversion from the Hg−dithiolate to Hg−trithiolate complex occurs with a pK_a of 8.6 for the **d** site which is one pK_a unit higher than the corresponding **a** site value of 7.6. The analysis of apo structures of (**CS**L9C)$_3$ and (**CS**L19C)$_3$ reveals that two thiols in each structure are at optimal distances of 4.58 and 4.64 Å, respectively, to accommodate Hg(II) in linear coordination, the ideal Hg−S distance for linear HgS_2 being 2.32 Å.[34] One of these thiols in each structure is oriented toward the interior of the helical scaffold and the other thiol to the helical interface. It is possible that linear coordination of Hg(II) in either **a** or **d** substituted peptides consists of these two types of thiols as ligating residues forming a preformed 2-coordinate site for Hg(II). Figure 7 shows the models of T-shaped Hg(II) complexes with **CS**L9C and **CS**L19C. It can be seen that the third thiol is at a distance of 4.31 and 3.33 Å from linear Hg(II) in (**CS**L9C)$_3$ and (**CS**L19C)$_3$, respectively. This difference in distances indicates that the geometry of the two T-shaped Hg-complexes are not same and may serve as structural models to explain the observed difference in [199]Hg NMR δ values between
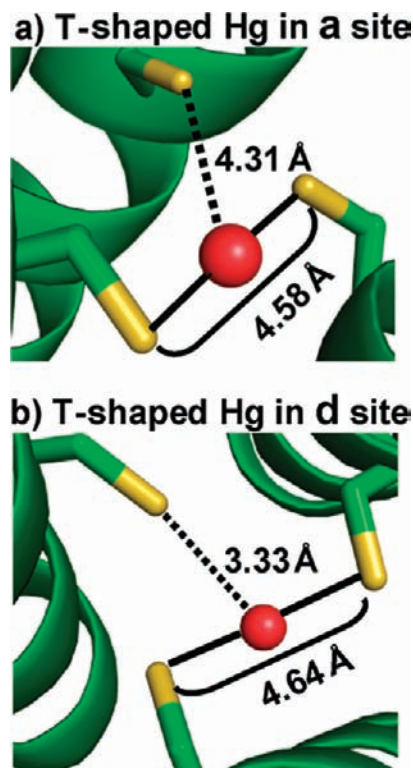

Figure 7. Models of T-shaped Hg(II) complexes inside three-stranded coiled coils. Shown are possible coordination modes of Hg(II) with the two thiols in (a) **CS**L9C and (b) **CS**L19C where one thiol is pointing toward the interior and the other toward the helical interface. Peptide backbone is shown as green ribbon, Cys residues as ball and stick, and Hg(II) as red sphere. Solid lines between sulfur atoms and Hg(II) in the two models represent S−Hg−S bonds; whereas the dotted lines from the third sulfur to the Hg(II) represent situations where this third sulfur may or may not be coordinated to the Hg(II) ion. With S−S separation of 4.58 and 4.64 Å, these two thiols are well suited to bind Hg(II) in linear coordination. The third thiol in **CS**L19C being at a shorter distance than in **CS**L9C may explain why Hg(II) in **d** sites is believed to be more T-shaped than in **a** site.

a and **d** sites. Our models from this study suggest that Hg(II) fits better in an **a** site as a trigonal HgS_3 at high pH than in a **d** site which is confirmed by [199]Hg NMR ($\delta = -185$ ppm for **a** site and $\delta = -313$ ppm for **d** site).[57,58] This observation may also serve as a plausible explanation for the higher pK_a for HgS_2−SH → HgS_3 complex formation for the **d** site compared to the **a** site. These structures provide important insight into explaining observed differences in metal binding to these sites in solution.

Presence of Zn(II) at the Crystal Packing Interfaces. Crystallization of **CS**L9C and **CS**L19C was not successful in the absence of Zn(II). Binding of Zn(II) to His and Glu residues at the crystal packing interfaces links the coiled coils together and provides a third dimension to the crystals and thus generates better diffraction quality crystals for X-ray studies. In the absence of Zn(II), however, 2D plate-like crystals are obtained which are not suitable for X-ray structural studies. As Zn(II) has intermediate polarizability (hard−soft character), it uses both hard ligands such as His, Glu, Asp and water molecules and soft ligands such as Cys in naturally occurring metalloproteins. However, in the majority (65%) of the Zn(II) containing metalloproteins, Zn(II) uses amino acids such as His, Glu, Asp,

(57) Iranzo, O.; Thulstrup, P. V.; Ryu, S.-B.; Hemmingsen, L.; Pecoraro, V. L. *Chem.−Eur. J.* **2007**, *13*, 9178−9190.

(58) Iranzo, O.; Ghosh, D.; Pecoraro, V. L. *Inorg. Chem.* **2006**, *45*, 9959−9973.

and water molecules as all of its first coordination sphere ligands.[59] Zn(II) binding to His and Glu residues and waters at the crystal packing interfaces of our peptides is not an exception of this later situation.

To examine the effect of external Zn(II) ions on the physical and spectroscopic properties of the bound metal at the designed metal binding site in solution, we have performed studies with **CSL9C** peptide and monitored the physical properties of Hg(II) in the presence of a varying concentration of Zn(II). Measures taken to remove ubiquitous Zn(II) ions from solution is described in the Materials and Methods. These studies were performed both at low pH, where the HgS_2 complex is formed within the three-stranded coiled, and at high pH where the HgS_3 complex is formed. Given that the solubility product[60] of $Zn(OH)_2$ is 2.1×10^{-16} and the high peptide concentrations (milimolar) used in the solution studies at low pH, experiments were not possible at pH values higher than 6.5 for the UV−vis and 5 for [199]Hg NMR experiments due to hydrolysis of Zn(II) leading to the formation of $Zn(OH)_2$ as precipitate. For the same reason, experiments at pH 8.6 where the HgS_3 complex is formed were not possible to perform above 10 μM **CSL9C** and 30 μM Zn(II) concentrations. Because of the low concentrations of peptide used at high pH experiments, it was not possible to obtain [199]Hg NMR measurements.

The UV−vis titration in Figure S7 of the Supporting Information shows that addition of up to 21 equiv of Zn(II) (per monomer) to 2.5 mM **CSL9C** in the presence of 1 equiv of Hg(II) (per trimer) at pH 6.5 does not seem to cause any changes in the HgS_2 signal at 247 nm as at this low pH condition Hg(II) coordinates to the peptide as linear HgS_2 within a three-stranded coiled coil.[34,57,58,61] The overall UV−vis spectra overlay very well in the presence of varying concentrations of Zn(II) except in the Trp absorbance region ∼280 nm. The crystallographic conditions for **CSL9C**/Zn(II) is 5.1/17 mM, that is, 1:3. For the UV−vis experiments, the **CSL9C**/Zn(II) ratio is 2.5/52.5 mM, that is, 1:21. Although the absolute concentration of the peptide is half that which is present in crystals, this data shows that a 7-fold relative excess of Zn(II) compared to the crystallographic conditions has no effect on binding of Hg(II) to **CSL9C**. Titration of Hg(II) to **CSL9C** in the presence of 21 equiv of Zn(II) (per monomer) (Supporting Information Figure S8, A) and in the absence of Zn(II) (Supporting Information Figure S8, B) shows that the stoichiometry of **CSL9C**/Hg(II) is unchanged (3:0.95) in the presence of Zn(II). Additionally, the molar extinction coefficient (2050 M^{-1} cm^{-1} at 247 nm) in the presence of Zn(II) is similar to the value of 2000 M^{-1} cm^{-1} observed in the absence of Zn(II). Similar values of molar extinction coefficient have been observed for linear HgS_2 within a three-stranded coiled coil for TRI peptides.[58,61] Hg(II) binding titration data both in the presence and absence of Zn(II) were analyzed by nonlinear least-squares fits. Because of strong binding, the minimum affinities obtained for Hg(II) binding to **CSL9C** in the presence and absence of Zn(II) are 1.4×10^7 M^{-1} and 2.3×10^7 M^{-1}, respectively. [199]Hg NMR chemical shift of 12 mM **CSL9C** and 252 mM Zn(II) (1:21 **CSL9C**/Zn(II), a 6-fold absolute excess of Zn(II) compared to crystallographic conditions) in the presence of 1 equiv of Hg(II) (per trimer) at

pH 5 is −926 ppm (Supporting Information Figure S9, A), expected for a T-shaped Hg(II) complex within a three-stranded coiled coil. The same chemical shift is observed under similar conditions in the absence of Zn(II) (Supporting Information Figure S9, B). These studies show that the presence of Zn(II) up to a concentration that is severalfold excess compared to what is present under crystallographic conditions does not influence the stoichiometry, affinity, and coordination number of Hg(II) bound at the designed metal site.

Titration of $HgCl_2$ to 10 μM **CSL9C** in 50 mM CHES buffer in the presence (Supporting Information Figure S10, A) and absence (Supporting Information Figure S10, B) of 30 μM Zn(OAC)$_2$ at pH 8.6 shows that the stoichiometry of **CSL9C**/Hg(II) is not influenced by the presence of 3-fold excess of Zn(II). The molar extinction coefficient of HgS_3 complex is similar in the presence and absence of Zn(II) at pH 8.6, the values being 18 000 and 19 500 M^{-1} cm^{-1}, respectively, at 247 nm. Hg(II) titration data were fit using nonlinear least-squares analysis. Because of strong binding, the minimum values of binding constants obtained are 6.6×10^7 and 4.3×10^7 M^{-1} in the presence and absence of Zn(II), respectively. These results show that the presence of a 3-fold excess of Zn(II) does not influence the stoichiometry and affinity of Hg(II) bound at the Cys site as HgS_3.

Conclusions

Having solved the crystal structures of apo **CSL9C**, an **a** site, apo **CSL19C**, a **d** site peptide, as well as our previously reported apo L-Pen (an analogue of Cys) and D-Pen **a** site structures, we are now in a unique position to evaluate the structural implications on modifying backbone chirality versus the subtle differences we have just reported between **a** versus **d** sites. At first glance, there is a striking similarity between the D-Pen in an **a** site and an L-amino acid (Cys) in a **d** site. Though these sites are not identical (most significantly the beta-C points toward the C-terminus for the D-amino acid), qualitatively, the orientation of thiols leads to larger thiol pockets in both the structures. From this similarity, one can envision that a D-amino acid in a **d** site may resemble an **a** site with L-amino acid. Furthermore, this approach may allow us to alter the various types of **a** versus **d** site specificity we have previously reported. Using the lessons learned from the structures of apo **CSL9C** and **CSL19C**, we have discussed the possible coordination modes in which heavy metals such as As(III) and Hg(II) can be sequestered by these peptides. Clearly, additional structures of metalated constructs would give direct evidence of the possible ways of metal coordination to these peptides. This article, which details the salient features of two *de novo* designed apo structures, can now serve as a basis for understanding solution behavior of metal encapsulation and physical properties of metallo derivatives of **Coil Ser** and related *de novo* designed family of peptides.

Materials and Methods

Peptide Synthesis and Purification. Peptides **CSL9C** and **CSL19C** were synthesized on an Applied Biosystems 433A automated peptide synthesizer using standard Fmoc protocols[62] and purified by reverse-phase HPLC on a C18 column at a flow rate of 10 mL/min using a linear gradient that was varied from 0.1% TFA in water to 0.1% TFA in 9:1 CH_3CN/H_2O over 50 min. Purified peptides were characterized by electrospray mass spectroscopy.

(59) Bertini, I. S. A.; Sigel, H. *Handbook of Metalloproteins*; Marcel Dekker, Inc.: New York, 2001.

(60) Ebbing, D. D.; Gammon, S. D. *General Chemistry*; 8th ed.; Houghton Mifflin: New York, Boston, 2008.

(61) Pecoraro, V. L. P.; Anna, F. A.; Iranzo, O.; Luczkowski, M. In *Bioinorganic Chemistry*; American Chemical Society: Washington, DC, 2009; pp 183−197.

(62) Chan, W. C.; White, P. D. *Fmoc Solid Phase Peptide Synthesis: A Practical Approach*; Oxford University Press: New York, 2000.

Crystallization. Crystals of **CS**L9C were grown by vapor diffusion on a hanging drop at 20 °C containing equal volumes (2 μL) of peptide (19.15 mg/mL **CS**L9C, 17 mM Zn(OAc)$_2$, 100 mM sodium cacodylate buffer at pH 6.0) and precipitant (100 mM Ca(OAc)$_2$ and 24% PEG 3350). Crystals were soaked in the mother liquor or cryoprotectant (20% ethylene glycol) prior to freezing in liquid N$_2$. **CS**L19C was crystallized by vapor diffusion in a sitting drop with equal volumes of peptide (10 mg/mL in 20 mM Zn(OAc)$_2$) and a precipitant solution (100 mM MES pH 6.5 and 40% PEG 200). The hexagonal plate-like crystals obtained were mounted in a 0.15 mm robotic loop and frozen in their mother liquor in liquid N$_2$ for data collection.

Data Collection and Refinement. Data were collected at the Advanced Photon Source of the Argonne National Laboratory on the LS-CAT Beamline 21-ID, equipped with a Mar 225 CCD detector. The 360° frames of data were collected with a rotation of 1° and exposure time of 1 s. The data were processed and scaled with HKL 2000.[63] The space group of **CS**L9C was determined to be *C*2. The structure of **CS**L9C was solved by molecular replacement using Phaser in CCP4 suite of programs[64,65] by using 29 amino acids of **CS**L16-L-Pen (PDB code 3H5F)[38] as the search model. Leu 9 of **CS**L16-L-Pen were mutated to Cys and the side chains of Pen 16 were modified in such a way that they resembled Leu residues containing only Cβ and Cγ atoms before using it as a search model for Molecular Replacement. The generated model was refined with restrained refinement by Refmac 5 in CCP4 suite of programs[66] and built in and completed in Coot[67] by using the $2F_o - F_c$ and $F_o - F_c$ electron density maps generated in Refmac 5. After one round of refinement, the methyl groups of Leu were built in using the density present in $F_o - F_c$ electron density map. The final structure was refined to 1.36 Å resolution ($R_{working}$ = 18.2%, R_{free} = 21.5%). The coordinates and structure factors of **CS**L9C have been deposited in the Protein Data Bank with the ID code 3LJM.

For **CS**L19C, the space group was determined to be *P*6$_1$ or *P*6$_5$. Molecular replacement with both potential space groups was performed in the program Phaser in the CCP4 suite of programs[64,65] with the first 26 amino acids of a single helix of Coil V$_a$L$_d$ (PDB code 1COI)[30] as a search model. The top 65% of rotation function solutions were included in the translation search. In two separate trials, three and six helices were searched for with zero allowed backbone clashes. The molecular replacement was successful for three helices per asymmetric unit in the space group *P*6$_1$ with a Z-score of 14.9 and a Log Likelihood Gain of 195. The Matthews coefficient was determined to be 3.65 which corresponded to a solvent content of 65%. The molecular replacement solution was used as input for the Auto Build feature of Phenix,[68] followed by refinement in Refmac.[66] $F_o - F_c$ and $2F_o - F_c$ electron density maps generated with the CCP4 map utility FFT and with the mtz phase file in Coot[50] were used for iterative building of side chains, Zn(II) ions, and water molecules. The structure was refined to 2.15 Å resolution ($R_{working}$ = 21.9%, R_{free} = 26.4%). The validity of the model was verified with a composite omit map generated in CNS.[69] The coordinates and structure factors of **CS**L19C have been deposited in the Protein Data Bank with the ID code 2X6P.

The data processing and refinement statistics for **CS**L9C and **CS**L19C are given in Table S1 and S2 in the Supporting Information. Figures were generated in Pymol.[70] Angles between thiol plane of **CS**L19C and planes formed by the C$_\gamma$ atoms of Leu 16 and Leu 23 were measured using the program Mercury from Cambridge Crystallographic Data Center.[71]

UV−Vis and ^{199}Hg NMR Spectroscopy. To remove ubiquitous Zn(II) from solution, peptide stock solutions and buffers were prepared in deionized water treated with Chelex-100 resin (BioRad). All plasticware and glassware were soaked in 5 mM EDTA overnight followed by several thorough rinses with deionized water. Only metal free pipet tips (Fisher) were used. All solutions were purged with argon before use to minimize chances of Cys oxidation. Peptide concentration was determined by quantization of Cys thiols using Ellman's test.[72] UV−vis experiments were performed at room temperature on a Cary 100 Bio spectrophotometer. Quartz cuvettes of path length 1 mm and 1 cm were used for the experiments at pH 6.5 and 8.6, respectively. Zn(II) titrations were performed by adding aliquots of 1 M stock solution of Zn(OAc)$_2$ to solutions containing 2.5 mM **CS**L9C and 50 mM MES buffer at pH 6.5 and 1 equiv of HgCl$_2$ (per trimer). Appropriate background spectrum was subtracted prior to addition of HgCl$_2$. Hg(II) titrations were performed by adding aliquots of 7.37 mM stock solution of HgCl$_2$ to solutions containing 2.5 mM **CS**L9C, 50 mM MES buffer at pH 6.5 in the presence of 21 equiv of Zn(OAc)$_2$ (per monomer) and with no Zn(II) present. For experiments at pH 8.6, same stock solution of HgCl$_2$ was added to solutions containing 10 μM **CS**L9C, 50 mM CHES buffer in the presence and absence of 30 μM Zn(OAc)$_2$. Direct Hg(II) titration data were analyzed by nonlinear least-squares fits to the equation similar to what has been described previously:[35,58]

$$A = \frac{1}{2K_b}\{K_bM_0 + K_bP_t + 1 - (K_b^2M_0^2 - 2K_b^2M_0P_t +$$
$$2K_bM_0 + K_b^2P_t^2 + 2K_bP_t + 1)^{1/2}b\Delta\varepsilon\}$$

where A is the observed absorbance on addition of Hg(II) to peptide solution, K_b is the binding constant of Hg(II) to be determined, P_t is the total concentration of peptide trimer, M_0 is the concentration of Hg(II) used during titration, $\Delta\varepsilon$ is the difference molar extinction coefficient of the complex formed during titration, and b is the path length of the cuvette. As the absorbance at 247 nm decreases in the presence of more than stoichiometric amount of Hg(II) due to formation of HgS$_2$ in two -stranded coiled coil, it was necessary to assume that the absorbance stays constant in order to fit the binding data. ^{199}Hg NMR experiments were performed at room temperature on a Varian Inova 500 spectrometer (89.5 MHz for ^{199}Hg) equipped with a 5 mm broadband probe as previously described.[73] The samples for ^{199}Hg NMR experiments contained (a) 12 mM **CS**L9C, 4 mM ^{199}Hg(NO$_3$)$_2$ (prepared from 91% isotopically enriched ^{199}HgO, Oak Ridge), 252 mM Zn(OAc)$_2$ and (b) 14 mM **CS**L9C and 4.6 mM ^{199}Hg(NO$_3$)$_2$. pH of both the samples was adjusted to 5 using concentrated solutions of KOH and HCl. pH of the solutions was also measured after the experiment. The

(63) Otwinowski, Z.; Minor, W. In *Methods in Enzymology: Macromolecular Crystallography, Part A*; Carter, C. W. J., Sweet, R. M., Eds.; Academic Press: New York, 1997; Vol. 276, pp 307−326.

(64) Potterton, E.; Briggs, P.; Turkenburg, M.; Dodson, E. *Acta Crystallogr, Sect. D* **2003**, *59*, 1131–1137.

(65) McCoy, A. J.; Grosse-Kunstleve, R. W.; Adams, P. V.; Winn, M. D.; Storoni, L. C.; Read, R. J. *J. Appl. Crystallogr.* **2007**, *40*, 658–674.

(66) Murshudov, G. N.; Vagin, A. A.; Dodson, E. J. *Acta Crystallogr., Sect. D* **1997**, *53*, 240–255.

(67) Emsley, P.; Cowtan, K. *Acta Crystallogr., Sect. D* **2004**, *60*, 2126–2132.

(68) Adams, P. D.; Grosse-Kunstleve, R. W.; Hung, L.-W.; Ioerger, T. R.; McCoy, A. J.; Moriarty, N. W.; Read, R. J.; Sacchettini, J. C.; Sauter, N. K.; Terwilliger, T. C. *Acta Crystallogr., Sect. D* **2002**, *58*, 1948–1954.

(69) Brunger, A. T.; Adams, P. D.; Clore, G. M.; DeLano, W. L.; Gros, P.; Grosse-Kunstleve, R. W.; Jiang, J.-S.; Kuszewski, J.; Nilges, M.; Pannu, N. S.; et al. *Acta Crystallogr., Sect. D* **1998**, *54*, 905–921.

(70) DeLano, W. L. *The PyMOL Molecular Graphics System*; DeLano Scientific: Palo Alto, CA, 2005; http://www.pymol.org.

(71) Macrae, C. F.; Bruno, I. J.; Chisholm, J. A.; Edgington, P. R.; McCabe, P.; Pidcock, E.; Rodriguez-Monge, L.; Taylor, R.; van de Streek, J.; Wood, P. A. *J. Appl. Crystallogr.* **2008**, *41*, 466–470.

(72) Ellman, G. L. *Arch. Biochem. Biophys.* **1959**, *82*, 70–77.

(73) Luczkowski, M.; Stachura, M.; Schirf, V.; Demeler, B.; Hemmingsen, L.; Pecoraro, V. L. *Inorg. Chem.* **2008**, *47*, 10875–10888.

data were analyzed using the software MestRe-C.[74] The free induction decay was processed by applying a linear prediction from 1 to 32 points out of 120 basis points with a coefficient of 32 followed by zero filling and exponential line broadening of 200 Hz prior to Fourier transformation.

(74) Cobas, C.; Cruces, J.; Sardina, F. J. ; 2.3 ed.; Universidad de Santiago de Compostela: Spain, 2000.

Supporting Information Available: Helical wheel diagrams of (**CSL9C**)$_3$, (**CSL19C**)$_3$, location of Zn(II) ions at crystal packing interfaces of (**CSL19C**)$_3$, orientation of Cys Sγ plane with respect to Leu 16 and Leu 23 layers of (**CSL19C**)$_3$, the overlay of α-helical backbones of (**CSL9C**)$_3$, (**CSL19C**)$_3$, (**CSL16-L-Pen**)$_3$ and (**CSL16-D-Pen**)$_3$, UV−vis titrations of Zn(II) to **CSL9C** and Hg(II), UV−vis titrations of Hg(II) to **CSL9C** in the presence and absence of Zn(II), and ^{199}Hg NMR spectra of **CSL9C** with ^{199}Hg(II) in the presence and absence of Zn(II). This material is available free of charge via the Internet at http://pubs.acs.org.

JA101812C